

Mass failures associated with the passage of a large tropical cyclone over the Swatch of No Ground submarine canyon (Bay of Bengal)

Kimberly G. Rogers and Steven L. Goodbred Jr.

Department of Earth and Environmental Sciences, Vanderbilt University, Nashville, Tennessee 37235, USA

ABSTRACT

Acoustic surveys collected six months before and after the passing of a major tropical cyclone over the Swatch of No Ground submarine canyon (Bay of Bengal) revealed the formation of widespread mass failures 30 km offshore of the Ganges-Brahmaputra river delta. Mass sediment flows several kilometers wide with minimal run-out distances (<300 m) are interpreted as liquefied strata that formed in response to hydrostatic loading and cyclic wave pumping during the storm. Several massive slide valleys (>1 km wide × 5–60 m thick) developed in areas with preexisting subsurface sediment deformation and evidence for active submarine fluid discharge. In contrast, narrow, steep-walled (7°–10°) gullies present before the storm did not fail, suggesting that the gully walls may be shear hardened by the preferential funneling of gravity flows from the Bengal shelf. Combined, the widespread mass failures and gullies are part of a rapidly accreting (5–50 cm/yr), net-aggradational canyon system that supports multiple mechanisms for sediment transport from the active river mouth to the canyon.

INTRODUCTION

Submarine mass failures are a principal mechanism in the evolution of continental margins, as their collapse dynamically impacts slope morphology while at the same time transporting sediment and sequestered carbon to the deep sea (McAdoo et al., 2000; Minisini and Trincardi, 2009). The most common triggers for mass failure in deep water include rapid sedimentation and seismic waves generated by earthquakes. Increased pore-pressure gradients due to submarine groundwater seepage, removal of overlying material, and diagenesis of organic matter can likewise weaken the shear strength of subsurface sediments, predisposing them to failure (Grozic, 2003; Orange and Breen, 1992). The mechanics behind these individual processes are well understood (e.g., Parsons et al., 2007), but a predictive understanding is limited by complex boundary conditions and a lack of observational field data.

Most studies of sediment mass failures have centered on the continental slope where such features are most common, particularly on widespread headless canyons and hazardous tsunamigenic slides (Parsons et al., 2007). Other research has focused on mass-transport processes that contribute to the evolution of shelf-indenting canyons, such as the updip propagation of failures on the upper slope and downcutting by turbidity currents (McAdoo et al., 2000; Pratson and Coakley, 1996; Twichell and Roberts, 1982). However, to date there is limited information on mass wasting processes within modern, actively accreting canyons that head in shallow water. Failures at the head of midshelf canyons can be triggered by the same mechanisms responsible for mass wasting at greater water depths, but shallow canyon heads are also susceptible to failure caused by cyclic wave pumping during the frequent passage of high-energy wind and storm events (Prior et al., 1989; Puig et al., 2004).

Toward a better understanding of how storms impact midshelf canyon processes, we present a pre- and post-storm comparison of morphologic features at the head of the Swatch of No Ground (SoNG) submarine canyon, which incises the Bengal shelf and active delta front of the Ganges-Brahmaputra river (Fig. 1). Two subbottom sonar surveys were conducted using a shallow-towed Edgetech 216s chirp system operated at a 2–10 kHz frequency in March 2007 and March 2008, six months

before and after a large tropical cyclone passed over the canyon. These data (1) allow an evaluation of the contribution of large storm events to midshelf canyon failure, (2) give rise to questions regarding areas of preferential failure within the upper canyon, and (3) highlight several factors influencing the magnitude and distribution of such failures. Finally, since the SoNG canyon head intercepts the actively prograding clinothem of the Ganges-Brahmaputra river delta (Michels et al., 2003), this research focuses on the canyon rim where transport-related features define the interactions between these two rapidly accreting depocenters (Kottke et al., 2003).

GEOMORPHIC SETTING AND CYCLONE SIDR

The SoNG incises 130 km onto the Bengal margin in a northeast-southwest direction, reaching within 30 km of the central delta coast of Bangladesh (Fig. 1). At the canyon head, which is ~150 km west of the active river mouth, radiometric dating (^{137}Cs , ^{210}Pb , and ^{228}Ra) yields sedimentation rates from ≥ 5 cm/yr along the canyon rim (20–40 mbsl [meters below sea level]) to extremely rapid rates of 20–50 cm/yr on the upper-canyon floor (~250 mbsl) (Kuehl et al., 1997; Kudrass et al., 1998; Michels et al., 2003). Based on these rates measured to the bottom of 5–10-m-long sediment cores, we estimate that the 20–30 m of strata imaged in our sonar records represent only 300–600 yr of sediment deposition, emphasizing that these are very young, thick, and likely underconsolidated deposits. With such rapid deposition, the canyon acts as a temporary sink for ~30% of the ~750 million metric tons of sediment delivered annually to the Bengal margin (Kuehl et al., 1997). The mass of sediment intercepted by the canyon represents 1%–2% of the global riverine sediment flux (Milliman and Syvitski, 1992); thus, mass failures in the SoNG may directly impact the fate of globally significant volumes of sediment.

On 15 November 2007, a tropical depression in the southern Bay of Bengal strengthened to form Cyclone Sidr, which tracked northward

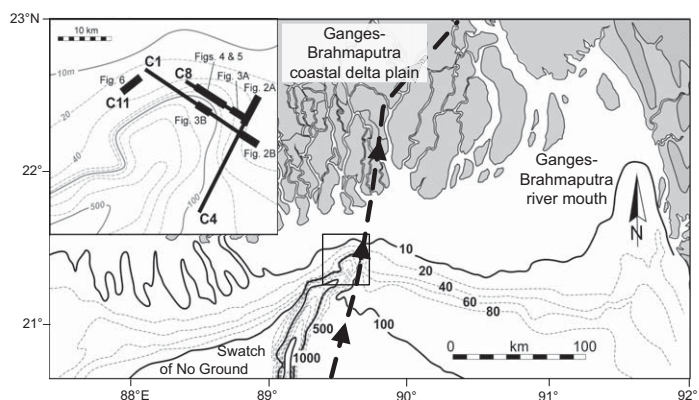


Figure 1. Bathymetric map of the Bengal shelf and upper Swatch of No Ground canyon, illustrating proximity to the Ganges-Brahmaputra river mouth estuary and coastal delta plain. Depths are in meters. Arrows and dashed line correspond to the track of Cyclone Sidr in mid-November 2007. Inset shows the location of the March 2007 and March 2008 chirp sonar survey lines and figures discussed in this paper. Lines of the two surveys are offset by no more than 50 m horizontal distance. (Figures 2–5 are provided in a separate insert accompanying this article.)

directly over the SoNG and struck the western coast of Bangladesh during an ebbing tide (Fig. 1). The system maintained wind speeds of 165 km/h for ~56 h before intensifying to 213 km/h near the Bengal margin, making it equivalent to a Category 5 tropical cyclone on the Saffir-Simpson scale. It was the second largest storm, based on wind speeds, to strike the Bangladesh coast since 1970. Tide gauge records indicate there was little surge near the SoNG, which was centered just west of the storm eye, but a significant 6–9 m surge did impact the coast to the east (Hasegawa, 2008). There are no observational wave data for this storm, as the nearest wave buoy (National Data Buoy Center [NDBC] Station 23101) is ~1200 km south of the Bangladesh coast. Cyclone Sidr was the only major cyclone in the Bay of Bengal between the two acoustic surveys, although a shallow-seated (~25 km deep) earthquake (M 5.2) occurred in southeastern Bangladesh on 7 November 2007. Earthquakes of this magnitude happen regularly in the region, and the epicenter of this modest event was located ~300 km away and was unlikely to have had an effect on the canyon.

MASS WASTING AND TRANSPORT-RELATED FEATURES

The general morphology and stratigraphy of the upper SoNG canyon (<120 mbsl) is dominated by clinof orm-like infilling, similar to that of the adjacent prograding delta front (Kuehl et al., 1997). This background morphology, however, is heavily punctuated by three types of geomorphic features, two of which are mass wasting structures associated with the passage of Cyclone Sidr, and the other a set of preexisting structures that remained mostly unchanged through the storm event (Table 1). The three features are defined as (1) mass flows—wide swaths of disturbed seabed and shallow strata that are characterized by modest run-out distances (10² m), the loss of all or most acoustic stratification (i.e., becoming acoustically transparent), and often by adjustment of the seabed to a horizontal surface of gravitational equipotential (Fig. 2¹); (2) slide valleys—broad, kilometer-wide depressions in which large, failed sediment blocks were vertically and horizontally displaced, either locally within the valley or considerably farther downslope (distance unknown) (Figs. 3–5 [see footnote 1]); and (3) gullies—relatively narrow (<300 m), steep-walled features scoured at their base and somewhat resistant to failure, remaining largely undisturbed following the cyclone (Figs. 4 and 5). Each of these geomorphic features are found throughout the upper canyon, where they occur as both spatially discrete entities and complex composites in which the different morphologies are superimposed or closely juxtaposed.

Mass Flows

Strata infilling gently sloping (<3°) portions of the canyon are acoustically well stratified, and parallel reflectors can be traced laterally for several kilometers. In post-storm survey data, this strong acoustic stratification locally disappears in the upper 2–6 m of sediments, coincident with a disturbance of the overlying seabed (Fig. 2 [see footnote 1]). Based on the coring of similar acoustically transparent beds, the sediment microfabric of these deposits shows that they have lost all physical bedding structure

(Kuehl et al., 2005). This loss of bedding, combined with downslope mass displacement and a disturbed seabed, suggests that these flows represent the liquefaction and/or fluidization of shallow strata associated with the storm event (the actual mechanics of these mass flows are indeterminate, but we refer to them here as liquefied flows to distinguish them from other types of mass flows). The liquefied beds and resulting flows commonly formed across several thousand meters of seabed, although they appear in the sonar data to have minimal run-out distances (i.e., <300 m) despite forming on sloped surfaces (0.3°–1.0°). Acoustically transparent beds similar to those associated with Sidr were also recognized in the pre-storm surveys, but most were overlain by several meters of stratified deposits presumably emplaced since a previous disturbance (storm?). Most mass flows formed in areas with apparent subsurface fluid escape structures connected to buried gassy deposits (Fig. 2).

Slide Valleys

Around the rim and head of the canyon, at least seven large valleys on the order of a kilometer wide were formed or reactivated by slide failures induced by the storm. Most occurred in areas of preexisting seabed and subbottom deformation, including abundant growth faults, linear or discrete acoustically transparent layers, and chaotic to subparallel strata. Many of the slide valley failures associated with Cyclone Sidr also show evidence for previous failure, with cycles of repeated collapse-and-infilling recognized through straight-walled slip planes that constrain decreasingly concave fill strata and overlying parallel beds, as well as acoustically transparent strata (Figs. 3A and 4–6 [see footnote 1]).

Although the SoNG slide valleys are all genetically related features, variation in their morphology appears to reflect different magnitudes of failure that we use to define three main types. In Type A valleys, the failed material is completely removed downslope (evacuated) to create a smooth U-shaped form with walls that dip ~6° (Figs. 4–6). The Type A features are the largest and most common of the valley failures, and they appear to account for the greatest volume of downslope-displaced sediment. Type B valleys are collapse features where large sediment blocks fail along high-angle slip planes (~7°–10°) with minimal downslope displacement (Fig. 3A). In all Type B cases, the post-storm valley remains at least partially filled by the failed material. The Type C valley is characterized by the complete evacuation of failed material like Type A, but the thickness of failed beds is comparatively thin (<10 m) resulting in the general preservation of pre-storm seafloor morphology (Fig. 3B). In addition, mass failure in the Type C valleys appears to be associated with the presence of fluid escape chimneys, as seen in the pre-storm sonar data (Fig. 3B). There is some evidence from intersecting sonar lines that these valley types are not mutually exclusive and may represent a continuum of genetically related morphologies.

Gullies

One of the most persistent features of the SoNG are steep-walled, relatively narrow gullies that originate on the inner shelf in water depths

TABLE 1. CHARACTERISTICS OF PRIMARY TRANSPORT-RELATED GEOMORPHIC FEATURES OBSERVED IN THE SWATCH OF NO GROUND CANYON FOLLOWING PASSAGE OF CYCLONE SIDR IN NOVEMBER 2007

Type of feature	Wall angle or surface gradient	Water depth to top of feature (m)	Thickness of failed beds (m)	Width of failure or gully (m)
Mass flows	0.3°–1.0°	35–115	2–6	2000–3500
Slide valleys (Type A—evacuated)	4°–8°	30–75	15–50	800–1300
Slide valleys (Type B—partially filled)	7°–10°	30–75	10–15	800–1200
Slide valleys (Type C—shallow failure)	6°–8°	100–150	5–10	400–700
Gullies	7°–10°	20–75	N.A.	200–300

¹Figures 2–5 are provided in a separate insert accompanying this article.

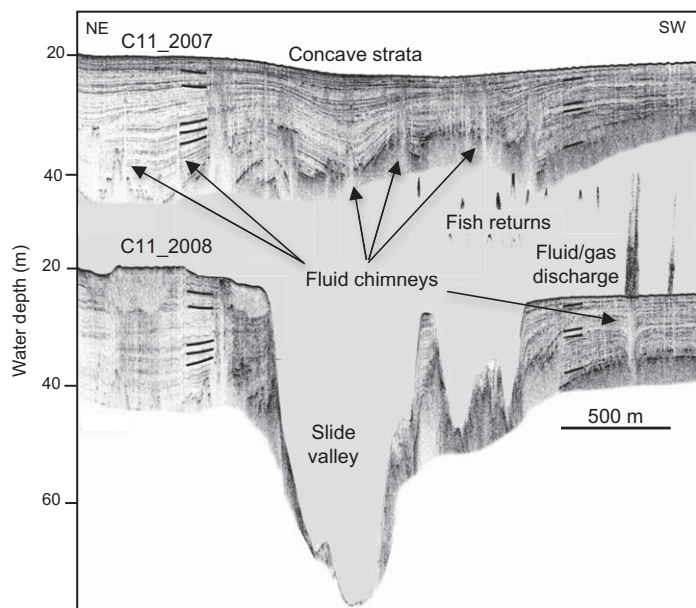


Figure 6. Comparison of pre- and post-storm sonar images from line C11 along the northwestern canyon rim, where both liquefaction flows and a massive Type A slide valley formed. Black lines highlight common stratal reflectors. Fish returns are acoustic reflections of fish in the water column. Sedimentation rates in this area are considerably lower than those in the eastern canyon (Michels et al., 2003), suggesting that rapid sedimentation is not a primary control on these failures. Rather, concave strata, shallow gas, and escape chimneys are all present at the failure site prior to the storm and appear strongly related to the style and location of failure. In the post-storm image, fluid discharge flares are observed by boosting the flat gain of the water-column sonar signal. These discharge flares demonstrate that the acoustically transparent chimney features connecting the seafloor and shallow strata with buried gassy sediments can serve as conduits for gas-charged submarine fluid escape and foci of large mass failures.

of 20 m. The relief of these features increases as they approach the canyon rim, reaching a maximum of ~20 m deep before debouching onto the low-gradient canyon floor (Figs. 3A, 4, and 5 [see footnote 1]). In both pre- and post-storm data, the steepest wall angles are consistently 7°–10°, slightly higher than those in most slide valleys. One or both gully walls are also typically draped with downlapping strata that reflect sediment aggradation. There are few signs of growth faulting or other penecontemporaneous deformation, and overall the gullies are stable and remained intact following passage of the storm.

DISCUSSION

Cyclone Sidr induced widespread mass wasting within the upper Swath of No Ground canyon, much of which was seemingly related to preexisting subsurface deformation and/or fluid/gas escape features. Other portions of the canyon remained relatively stable through the storm and were characterized by a lack of preexisting strata deformation. Together, both failures (i.e., mass flows and slide valleys) and persistent geomorphic features (i.e., gullies) define distinct sediment-transport pathways from the inner shelf to the central canyon, and perhaps to the deep-sea Bengal fan. In the absence of dynamical observations, though, we are informed about their controls and mechanisms principally through the pre-storm and post-storm acoustic surveys.

In this case the shallow-water, steep-walled gullies that resisted failure help define the stability threshold of cohesive sediments that are rapidly accumulating at the canyon head. In comparison to the fault-ridden slide valleys, the steeper-walled gullies lack growth faults or other styles

of deformation. Furthermore, strata downlapping onto the gully walls suggest that the gullies were not formed by incision, but rather are part of a vertically aggrading, net-depositional transport system (Figs. 4 and 5 [see footnote 1]) (Straub and Mohrig, 2009). This vertical translation of the gully form is supported by horizontally stratified sediments that tightly bound the gullies far below their current depth, indicating that the gully forms have been aggrading at their present location for perhaps several hundred years. We speculate that the resistance of the gullies to Sidr-related failure was sustained in part by the shear hardening of accumulated sediments through regular conveyance of shelf- or locally-sourced gravity flows (Parchure and Mehta, 1985; Kudrass et al., 1998).

In contrast to the quasi-stable gullies, widespread mass flows occur even on low gradients around the canyon rim and adjacent shelf, and their limited downslope displacement suggests that oversteepening is not a principal cause of failure. The presence of previously liquefied beds (i.e., acoustically transparent layers) within low-gradient strata beneath many of those associated with Cyclone Sidr indicates that liquefaction may occur repeatedly at the same locations. In general, the shallow mass flows observed around the SoNG and adjacent Bengal shelf are not unlike storm-induced mass flows described from other accreting shallow-water delta fronts (e.g., Mississippi; Prior and Coleman, 1978).

Together, the coincident formation of both shallow mass flows and the deeper-seated slides suggests a common trigger for the two types of failures, most likely wave pumping and related hydrodynamic loading during passage of the storm (Clukey et al., 1985; Prior et al., 1989; Puig et al., 2004). What then accounts for the very different morphology of these two failure types, particularly the 10–50 m thickness of failed strata in the slide valleys, which are uniquely large for high-energy, shallow-water settings? We propose that the greater failure depth of the slide valleys involves an additional control in which subbottom fluids, gas, and/or underlying morphology play a key role in defining the deep-seated base of these features. This hypothesis emerges from ideas on the origin of headless canyons that are nearly ubiquitous along the world's continental slopes (Twichell and Roberts, 1982; Surpless et al., 2009), where there is strong support that stratigraphically controlled subbottom fluid transport can lead to their formation and longer-term maintenance (e.g., Orange and Breen, 1992). Although these ideas are not fully tested in the SoNG, the pre- and post-storm surveys presented here may yield relevant insights on the relationship between submarine groundwater, mass failures, and margin morphology.

Specifically for the SoNG slide valleys, evidence for a subbottom control on the depth of failure emerges from observations of pre- and post-storm submarine fluid discharge at failure sites (Fig. 6), and of active sediment deformation with apparently repeated cycles of failure-and-infilling. Evidence for abundant submarine groundwater discharge along the Bengal margin has been revealed through geochemical tracers in the coastal ocean (e.g., ^{226}Ra , Ba, $^{87}\text{Sr}/^{86}\text{Sr}$), with estimates of fluid flux on the same order as surface-water discharge from the Ganges-Brahmaputra river (Moore, 1997; Basu et al., 2001). The specific processes and magnitude of coastal groundwater discharge remain uncertain (Harvey et al., 2002), but laterally extensive coarse-grained fluvial deposits infilling the lowstand river valleys are ideal candidates for groundwater conduits between the delta plain and the Bengal shelf (Moore, 1999). Indeed, sandy braided river deposits that are 30 to >50 m thick and tens of kilometers wide underlie most of the prograding coastal plain muds of the delta front (Goodbred and Kuehl, 2000). These deposits presumably extend 30 km offshore to the canyon head, where the buried lowstand river valleys intersect the larger SoNG canyon system.

We hypothesize that the sapping of submarine groundwater at the interface of the buried braided river sands and younger clinotherm muds generates high pore pressure along the canyon walls that, coupled with the storm surge and wave pumping, resulted in the deep-seated failures

that characterize the slide valleys. Evidence for active submarine fluid escape in and around the valley failures includes discharge “flares” that are visible in the water column when the sonar’s acoustic gain is increased (Fig. 6). Similarly, dense fields of fluid “chimneys” can be seen to bisect the upper 5–10 m of canyon strata at many failure locations (Figs. 2 and 3B [see footnote 1]). Overall, the widespread occurrence of submarine fluids discharging at the canyon head could help explain how the SoNG has maintained its relative nearshore position through the late Holocene despite very high rates of sedimentation.

CONCLUSIONS

Widespread mass failures around the head and rim of the SoNG canyon appear to have been triggered by passage of an intense tropical cyclone. Numerous liquefied or fluidized mass flows account for local redistribution of the upper 5–6 m of sedimentary strata, presumably induced by cyclic wave pumping during the storm. Other deep-seated failures formed large slide valleys more than a kilometer wide and tens of meters deep. Formation of these slide valleys appears to be associated with active submarine fluid discharge, possibly emerging where the canyon head intersects buried sandy fluvial strata. Overall, the mechanisms and scales of failure in the SoNG canyon, particularly the slide valleys, have not been previously documented for such a shallow-water, nearshore setting. Continued development of these pre- and post-storm acoustic data sets from the Bengal margin will be aimed at defining the processes and controls of sediment exchange between the prograding delta front and actively accreting canyon.

ACKNOWLEDGMENTS

We would like to thank Sirajur Rahman Khan (Geological Survey of Bangladesh), Emdadul Haque (Bangladesh Inland Waterways Transportation Authority), and the crew of the R/V *Dishari*. We are grateful for the helpful suggestions of K.M. Straub and two anonymous reviewers. This research was funded through National Science Foundation grant OCE-0630595.

REFERENCES CITED

Basu, A.R., Jacobsen, S.B., Poreda, R.J., Dowling, C.B., and Aggarwal, P.K., 2001, Large groundwater strontium flux to the oceans from the Bengal Basin and the marine strontium isotope record: *Science*, v. 293, p. 1470–1473, doi: 10.1126/science.1060524.

Clukey, E.C., Kulhawy, F.H., Liu, P.L.F., and Tate, G.B., 1985, The impact of wave loads and pore-water pressure generation on initiation of sediment transport: *Geo-Marine Letters*, v. 5, p. 177–183, doi: 10.1007/BF02281636.

Goodbred, S.L., Jr., and Kuehl, S.A., 2000, The significance of large sediment supply, active tectonism, and eustasy on margin sequence development: Late Quaternary stratigraphy and evolution of the Ganges-Brahmaputra delta: *Sedimentary Geology*, v. 133, p. 227–248, doi: 10.1016/S0037-0738(00)00041-5.

Grozic, J.L.H., 2003, Liquefaction potential of gassy marine sands, in Locat, J., and Mienert, J., eds., *Submarine mass movements and their consequences*: Dordrecht, Netherlands, Kluwer Academic Publishers, p. 37–45.

Harvey, C.F., Basu, A.R., Jacobsen, S.B., Poreda, R.J., Dowling, C.B., and Aggarwal, P.K., 2002, Groundwater flow in the Ganges delta: *Science*, v. 296, p. 1563, doi: 10.1126/science.296.5573.1563a.

Hasegawa, K., 2008, Features of super cyclone SIDR to hit Bangladesh in Nov., 07 and measures for disaster—From results of JSCE investigation: Sapporo, Japan, Foundation of River & Watershed Environment Management, p. 51–59.

Kottke, B., Schwenk, T., Breitzke, M., Wiedicke, M., Kudrass, H.R., and Spiess, V., 2003, Acoustic facies and depositional processes in the upper submarine canyon Swatch of No Ground (Bay of Bengal): *Deep-Sea Research Part II: Topical Studies in Oceanography*, v. 50, p. 979–1001, doi: 10.1016/S0967-0645(02)00616-1.

Kudrass, H.R., Michels, K.H., Wiedicke, M., and Suckow, A., 1998, Cyclones and tides as feeders of a submarine canyon off Bangladesh: *Geology*, v. 26, p. 715–718, doi: 10.1130/0091-7613(1998)026<0715:CATAFO>2.3.CO;2.

Kuehl, S.A., Levy, B.M., Moore, W.S., and Allison, M.A., 1997, Subaqueous delta of the Ganges-Brahmaputra river system: *Marine Geology*, v. 144, p. 81–96, doi: 10.1016/S0025-3227(97)00075-3.

Kuehl, S.A., Allison, M.A., Goodbred, S.L., and Kudrass, H.-R., 2005, The Ganges-Brahmaputra delta, in Giosan, L., and Bhattacharya, J., eds., *Deltas—Old and new*: SEPM (Society for Sedimentary Geology) Special Publication 83, p. 413–434.

McAdoo, B.G., Pratson, L.F., and Orange, D.L., 2000, Submarine landslide geomorphology, US continental slope: *Marine Geology*, v. 169, p. 103–136, doi: 10.1016/S0025-3227(00)00050-5.

Michels, K.H., Suckow, A., Breitzke, M., Kudrass, H.R., and Kottke, B., 2003, Sediment transport in the shelf canyon “Swatch of No Ground” (Bay of Bengal): *Deep-Sea Research Part II: Topical Studies in Oceanography*, v. 50, p. 1003–1022, doi: 10.1016/S0967-0645(02)00617-3.

Milliman, J.D., and Syvitski, J.P.M., 1992, Geomorphic/tectonic control of sediment discharge to the ocean: The importance of small mountainous rivers: *Journal of Geology*, v. 100, p. 525–544, doi: 10.1086/629606.

Minisini, D., and Trincardi, F., 2009, Frequent failure of the continental slope: The Gela Basin (Sicily Channel): *Journal of Geophysical Research*, v. 14, F03014, doi: 10.1029/2008JF001037.

Moore, W.S., 1997, High fluxes of radium and barium from the mouth of the Ganges-Brahmaputra River during low river discharge suggest a large groundwater source: *Earth and Planetary Science Letters*, v. 150, p. 141–150, doi: 10.1016/S0012-821X(97)00083-6.

Moore, W.S., 1999, The subterranean estuary: A reaction zone of ground water and sea water: *Marine Chemistry*, v. 65, p. 111–126, doi: 10.1016/S0304-4203(99)00014-6.

Orange, D.L., and Breen, N.A., 1992, The effects of fluid escape on accretionary wedges 2: Seepage force, slope failure, headless submarine canyons, and vents: *Journal of Geophysical Research*, v. 97, p. 9277–9295, doi: 10.1029/92JB00460.

Parchure, T.M., and Mehta, A.J., 1985, Erosion of soft cohesive sediment deposits: *Journal of Hydraulic Engineering*, v. 111, p. 1308–1326, doi: 10.1061/(ASCE)0733-9429(1985)111:10(1308).

Parsons, J.D., Friedrichs, C.T., Traykovski, P.A., Mohrig, D., Imran, J., Syvitski, J.P.M., Parker, G., Puig, P., Buttle, J.L., and Garcia, M.H., 2007, The mechanics of marine sediment gravity flows, in Nittrouer, C.A., et al., eds., *Continental margin sedimentation: From sediment transport to sequence stratigraphy*: International Association of Sedimentologists Special Publication 37, p. 275–338.

Pratson, L.F., and Coakley, B.J., 1996, A model for the headward erosion of submarine canyons induced by downslope-eroding sediment flows: *Geological Society of America Bulletin*, v. 108, p. 225–234, doi: 10.1130/0016-7606(1996)108<0225:AMFTHE>2.3.CO;2.

Prior, D.B., and Coleman, J.M., 1978, Disintegrating retrogressive landslides on very-low-angle subaqueous slopes, Mississippi delta: *Marine Georesources and Geotechnology*, v. 3, no. 1, p. 37–60, doi: 10.1080/10641197809379793.

Prior, D.B., Suayda, J.N., Lu, N.-Z., Bornhold, G.H., Keller, G.H., Wiseman, W.J., Wright, L.D., and Yang, Z.-S., 1989, Storm wave reactivation of a submarine landslide: *Nature*, v. 341, p. 47–50, doi: 10.1038/341047a0.

Puig, P., Ogston, A.S., Mullenbach, B.L., Nittrouer, C.A., Parsons, J.D., and Sternberg, R.W., 2004, Storm-induced sediment gravity flows at the head of the Eel submarine canyon, northern California margin: *Journal of Geophysical Research*, v. 109, C03019, doi: 10.1029/2003JC001918.

Straub, K.M., and Mohrig, D., 2009, Growth of constructional canyons via sheet flow turbidity currents: Observations from offshore Brunei Darussalam: *Journal of Sedimentary Research*, v. 79, p. 24–39, doi: 10.2110/jsr.2009.006.

Surpless, K.D., Ward, R.B., and Graham, S.A., 2009, Evolution and stratigraphic architecture of marine slope gully complexes: Monterey Formation (Miocene), Gaviota Beach, California: *Marine and Petroleum Geology*, v. 26, no. 2, p. 269–288, doi: 10.1016/j.marpetgeo.2007.10.005.

Twicheil, D.C., and Roberts, D.G., 1982, Morphology, distribution, and development of submarine canyons on the United States Atlantic continental slope between Hudson and Baltimore Canyons: *Geology*, v. 10, p. 408–412, doi: 10.1130/0091-7613(1982)10<408:MDADOS>2.0.CO;2.

Manuscript received 3 March 2010

Revised manuscript received 8 June 2010

Manuscript accepted 11 June 2010

Printed in USA

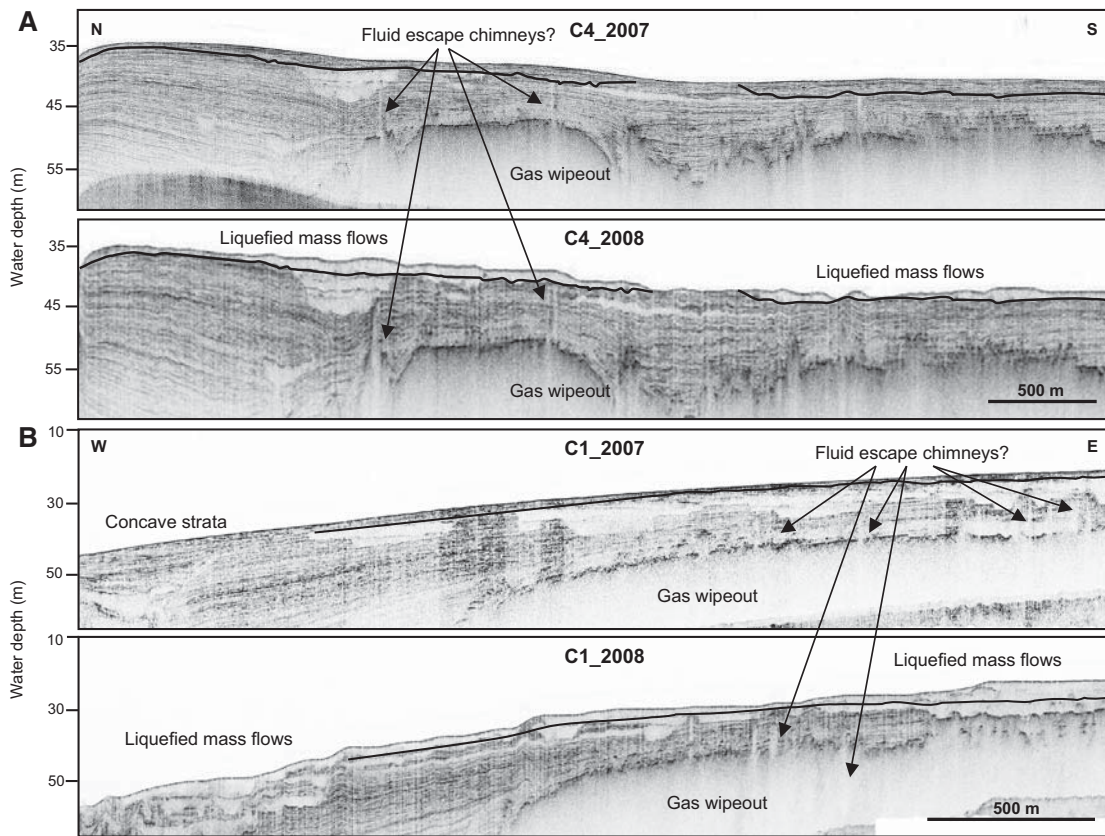


Figure 2. Comparison of pre- and post-storm sonar images from lines C4 and C1, showing thin (2–6 m), shallowly buried acoustically transparent sediments that serve as the foci of liquefied mass flows associated with Cyclone Sidr. For reference between the two surveys, the black lines highlight common stratal reflectors. A: Vertical, acoustically transparent striations appear to be gas/fluid escape “chimneys” originating in buried gassy sediments. The seafloor and shallow strata above these chimneys appear to preferentially fail during the storm. B: Similar to the flows in C4, mass failures appear to be associated with chimney structures originating in gassy sediments. The mass flows in the western portion of the image occur where the underlying pre-storm strata are increasingly concave, suggesting that some areas may experience repeated cycles of failure and infilling, or are deforming penecontemporaneously with rapid sediment deposition.

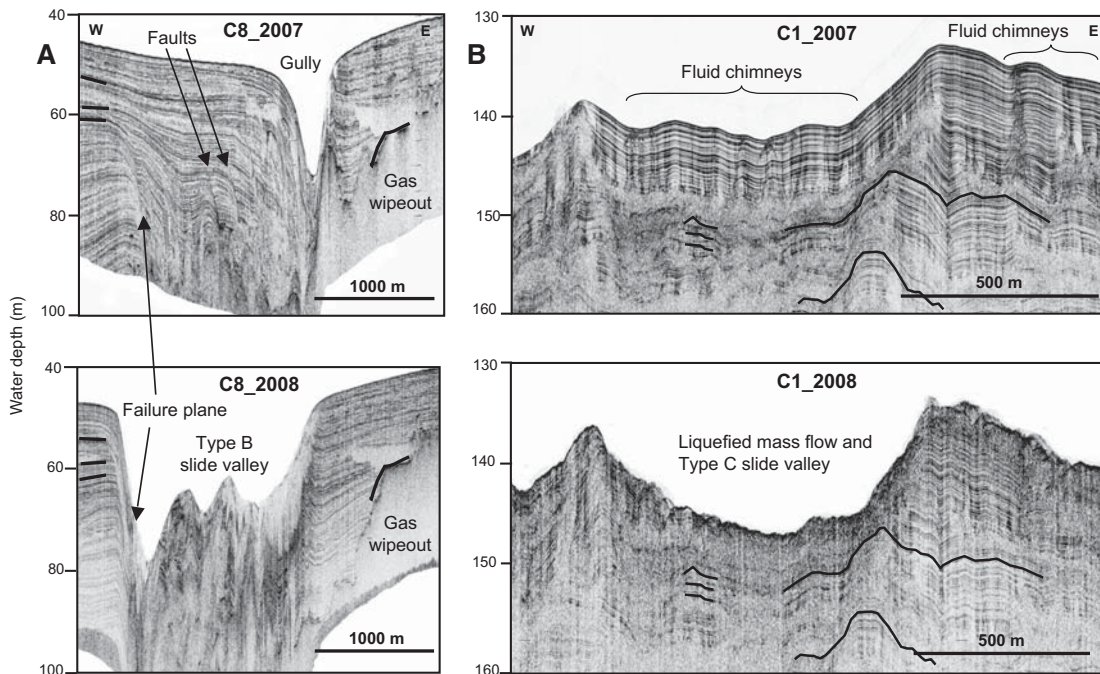


Figure 3. Comparison of pre- and post-storm sonar images from lines C8 and C1 showing the formation of Type B and Type C slide valleys. For reference between the two surveys, the black lines highlight common stratal reflectors. A: From line C8 a gully with strata downlapping its western wall is the dominant geomorphic feature prior to the storm, although faults, concave strata, and gas wipeouts are prominent in the subsurface. The 2008 survey shows the slide valley failed along a preexisting fault plane to form its western margin, and the former gully comprises the eastern wall. Failed sediments are not completely evacuated and partially fill the slide valley (Type B). B: From line C1 a shallow-seated Type C slide valley forms where the upper 5–6 m of acoustically stratified sediments failed. The failure preferentially occurred where the pre-storm strata are heavily bisected by fluid-escape chimneys. These escape structures connect buried gassy sediments to the seabed, and many of them display strong parabolic reflectors, suggesting gas ebullition during fluid escape.

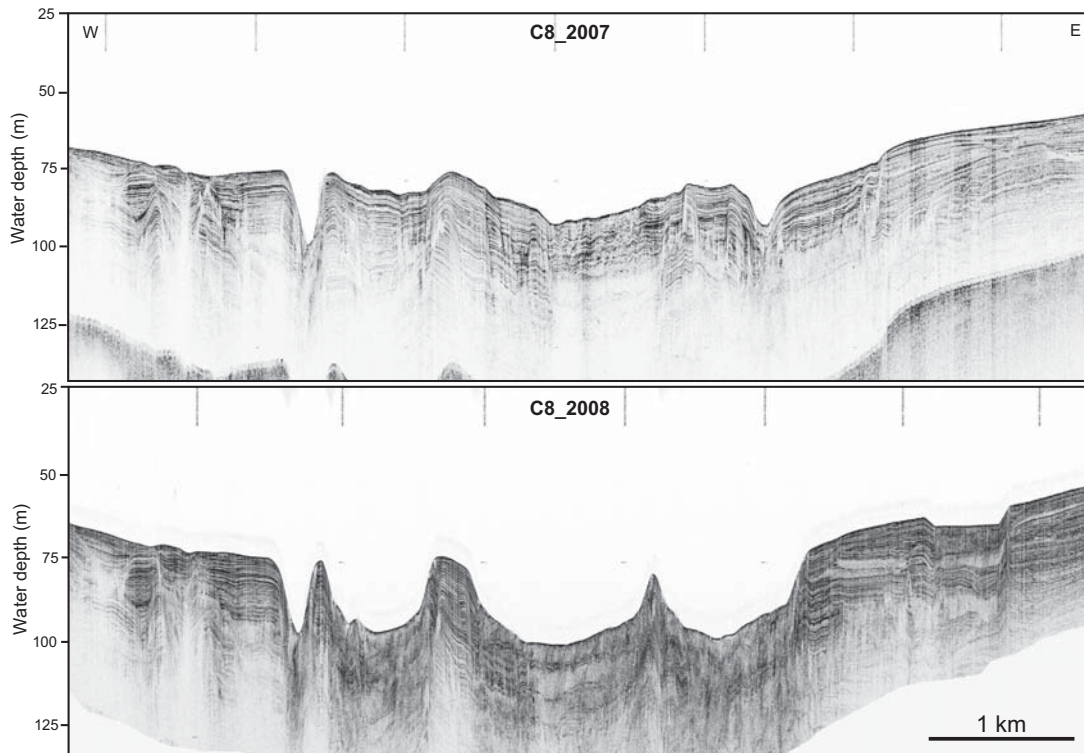


Figure 4. Uninterpreted pre- and post-storm chirp sonar line C8 across the head of the canyon. Preexisting subsurface deformation and examples of typical steep-walled gullies and zones of stability that resisted Sidr-related failure can be seen in the pre-storm line (compare to Fig. 5).

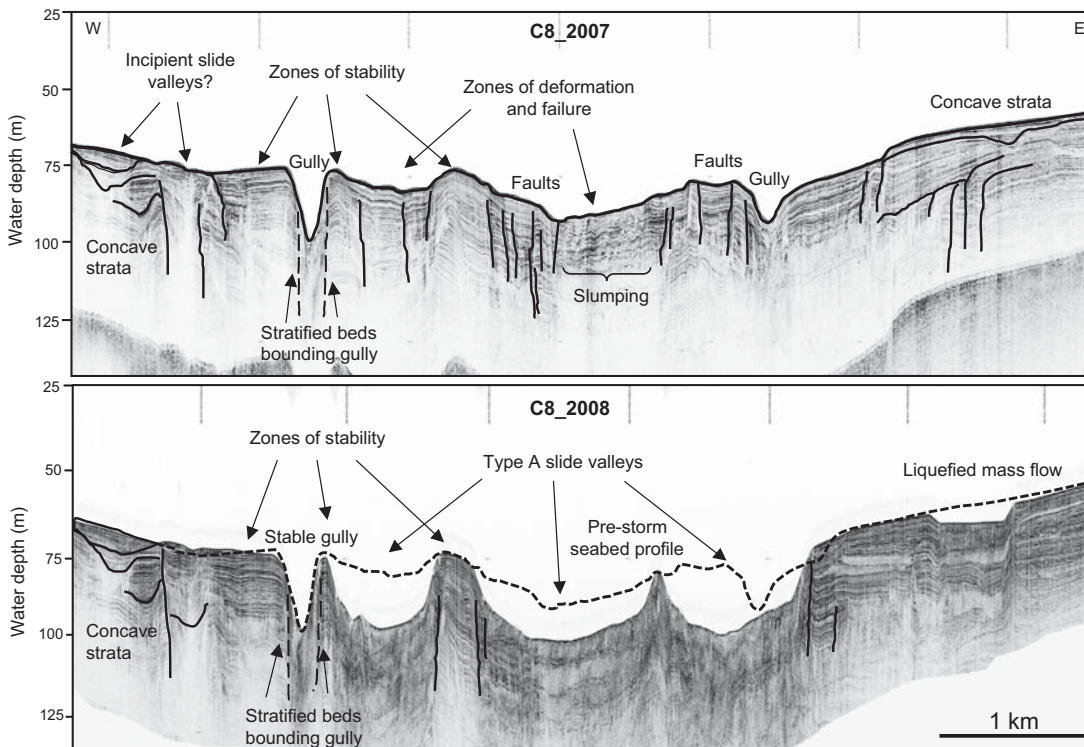


Figure 5. Interpreted pre- and post-storm chirp sonar line C8. The pre-storm seafloor profile has been overlaid on the post-storm image to highlight the magnitude of changes to the seabed. In the pre-storm example, slumping, faulting, and localized zones of concave strata overlain by parallel bedding are indicated. Three zones of stable seabed that maintained stratal integrity and resisted failure during the storm are also marked. Failure of sediment created large evacuated slide valleys (Type A), the floors of which are capped with >6-m-thick acoustically transparent sediments. Minimal stratification was preserved on the walls or at the base of new valley floors. While the westernmost gully remained intact, the easternmost gully collapsed into a slide valley (compare to gully in Fig. 3A, which is also from C8 and ~1 km east of Fig. 5). Concave strata on the eastern portion of the profile also failed as a 500-m-wide mass flow that formed ~3–5 m scarps on each side and leveled out to the gravitational equipotential surface. The loss of mass is presumed to reflect material that liquefied and flowed toward the canyon base. Concave strata on the western portion of the profile did not fail, although this area may be the site of future failure.